Volume 7, Issue 4, 2017, 2108 - 2116 ISSN 2069-5837

Biointerface Research in Applied Chemistry

www.BiointerfaceResearch.com

Original Research Open Access Journal

Received: 24.06.2017 / Revised: 28.07.2017 / Accepted: 30.07.2017 / Published on-line: 15.08.2017

Monomethyl polyethylene glycol modified oleanolic acid, synthesis, characterization and binding to bovine serum albumin

Xingjia Guo [1], Xiangjun Zhang [2], Jie Yao [1], Liping Xu [1], Lizhi Zhang [1], Xiangming Wang [1], Aijun Hao [3, *]

[1] College of Chemistry, Liaoning University, Shenyang 110036, P.R. China
[2] Shandong Institute of Pharmaceutical Industry, Jinan 250101, P.R. China
[3] College of Pharmacy, Liaoning University, Shenyang 110036, P.R. China

*corresponding author e-mail address: ***haoaj2012@hotmail.com***

ABSTRACT

In this paper, monomethyl polyethylene glycol (mPEG) modified oleanolic acid (mPEG-OA) was prepared by esterifying oleanolic acid with mPEG and characterized by UV-vis absorption, FITR, NMR and gel permeation chromatography (GPC). The interaction of mPEG-OA and bovine serum albumin (BSA) was investigated by fluorescence quenching, UV-vis absorption, FTIR and circular dichroism (CD) under the simulated physiological conditions. The results indicate that mPEG-OA quench the intrinsic fluorescence of BSA via a dynamic quenching process with the binding constant (*Ka*) in the order of 10^3 L/mol. The thermodynamic parameters suggest that the binding reaction mainly is driven by hydrophobic forces and belonged to a spontaneous process. The average binding distance between mPEG-OA and the tryptophan (Trp) residue of BSA was 3.5 nm. The probe displacement experiments confirmed that mPEG-OA mainly binds to sub-domain II A (site I) of BSA. The results of synchronous fluorescence, FTIR and CD spectra revealed that the binding process of mPEG-OA with BSA did not induce significant changes in the secondary structure as well as the polarity of the region around the Trp and Tyr residues in BSA.

Keywords: *Oleanolic acid, Monomethyl polyethylene glycol, conjugate, bovine serum albumin, binding interaction.*

1. INTRODUCTION

Oleanolic acid (OA) is one of bioactive pentacyclic triterpenoids, which exits widely in a lot of food or many Asian herbs, such as *fructus ligustri lucidi*, *fructus orsythiae*, and *akebia trifoliate* [1, 2]. It has been well documented that OA possesses many bioactivities, such as anti-inflammatory, antioxidant and anticancer activity[3]. But the low aqueous solubility (<1 μg/ml)[4], low permeability and lower oral bioavailability of around 0.7% seriously limit its further application [5]. Therefore, many OA derivatives have been investigated for improving its the potential pharmacological potencies [6].

Recently, modification insoluble drugs with hydrophilic polymer polyethylene glycol (PEG) have drawn great attentions in the field of biomedicine, because of significantly improving their bioavailability, extending their physiological stability in circulatory system and reducing its immunogenicity[7, 8]. Therefore, in this contribution mPEG-OA was synthesized and interaction with BSA was investigated.

Serum albumin possesses a wide variety of functions such as the maintenance of oncotic pressure, the clearance of reactive oxygen and nitrogen species, the inhibition of platelet aggregation and anticoagulation [9]. Serum albumins play important roles, which affect *in vivo* and *in vitro* behaviors of drugs in plasma. The interaction between drugs and proteins, especially serum albumins, will significantly affect the apparent distribution volume and the clearance rate of drugs in blood plasma [10]. Thus, the binding studies of drugs and serum albumins can provide important information about not only the relationship between chemical structure and pharmacologic activity[11-13], but also influence on the structure and function of protein [14].

Bovine serum albumin (BSA) is frequently selected as protein model in biomedicine field because of ready availability, low cost, ligand binding properties and particularly its structural homology with human serum albumin [15, 16]. BSA molecule consists of three linearly arranged, structurally homologous domains (I–III) and each domain includes two sub-domains (A, B) and the principal drugs binding sites were situated within the hydrophobic cavities (sites I and II) [17]. It has been verified that some compounds possess site specific binding ability to serum albumin and are often used as site probes, for example, phenylbutazone and ketoprofen in site I, flufenamic acid and ibuprofen in site II [18]. Two tryptophan residues (Trp-134 and Trp-212) in BSA possess intrinsic fluorescence and are often used to measure the drug-binding affinity [18].

In this paper, mPEG-OA compound was prepared according to previously reported method with slight modification [19], and the interaction between mPEG-OA and BSA was investigated using several spectroscopic techniques. The quenching mechanism and the conformational changes of mPEG binding to BSA were explored. Cheng and his co-workers have studied the interaction of BSA and OA [20], but no report is found concerning the binding reaction of BSA and mPEG-OA. The study is expected to provide some beneficial information for designing and screening new OA derivatives.

2. EXPERIMENTAL SECTION

2.1. Chemicals. Bovine serum albumin (fatty acid free, purity□98%) was purchased from Sino-American Biotechnology Company (China). Phenylbutazone, ibuprofen and oleanolic acid were obtained from the National Institute for Food and Drug Control (China). mPEG (Mw 2000) was purchased from Sigma-Aldrich and vacuum dried before used. The other chemicals were of analytical reagent grade without further purification. Double distilled water (DDW) was used throughout the experiments.

2.2. Apparatus. Fluorescence spectra were recorded on a Cary Eclipse 300 FL spectrophotometer (Varian Company, USA) equipped with a thermostat bath and 1.0 cm quartz cells, and the excitation and emission slits were set at 5 nm with the scanning rate of 1200 nm·min-1. All UV–vis absorption spectra were measured on a Cary 5000 UV–vis spectrophotometer (Varian Company, USA) equipped with 1.0 cm quartz cells. CD spectra were scanned on JASCO-J-810 circular dichroism spectrometer (JASCO, Japan) using a 1.0 cm quartz cell. The average molecular weight of mPEG-OA was determined by GPC column (HT3, Waters) equipped with a Waters-1515 bump (Waters Corporation, USA) and a differential refraction detector (Waters 2414). All pH measurements were performed on a pHS-3 digital pH-meter (Shanghai Selon Scientific Instrument Co., Ltd., China). FTIR spectra were recorded at room temperature on a Nicolet Nexus 670 FTIR spectrometer (Thermo Nicolet Company, USA) equipped with a germanium attenuated total reflection (ATR), deuterated triglycine sulphate (DTGS) detector and a KBr beam splitter. 1H NMR spectra were performed on nuclear magnetic resonance spectrometer (Mercury 300, Varian Company, US). The FTIR spectra for OA, mPEG, mPEG-SA, and mPEG-OA compounds were recorded in the spectral region of 4000-400 cm–1 in a KBr pellet with a 4 cm-1 resolution at room temperature, respectively.

2.3. Preparation of mPEG-OA. mPEG-OA was prepared using succinic anhydride as linker, according to the method previous reported with a slight modification[19]. The synthetic route of mPEG-OA was depicted in Scheme 1. Firstly, mPEG succinate acid (mPEG-SA) was prepared by esterification reaction of mPEG and succinic anhydride with pyridine as catalyst in chloroform. mPEG succinyl chloride (MPEG-SC) is prepared from mPEG-SA to increase its reaction activity, which will further react with OA to obtain mPEG-OA. Typically, 1.0 g of mPEG-SA was added into a three-necked, round-bottom flask equipped with a magnetic stirrer and a water-cooled reflux condenser. 10 mL of thionyl chloride was slowly added from a dropping funnel. Hydrogen chloride gas generated was absorbed through an absorption bottle containing NaOH solution. The reaction mixture was heated at reflux for 2 hr under stirring. After evaporation of the excess thionyl chloride, mPEG-SC residue was dissolved in 10 mL dry tetrahydrofuran (THF) for the next step.

0.500 g of OA was dissolved in 40 mL dry THF and stirred in an ice-cold water bath. 0.050 g of anhydrous potassium carbonate (K2CO3) was added to the OA solution. mPEG-SC in 10 mL THF was added into OA solution dropwise within 20 min under continuous stirring. The mixture was stirred for 2 h in an ice-cold water bath, another 2 h under room temperature, and heated up to 50℃ for 4 h. After then, solvent was evaporated and concentrated to about 10 mL under reduced pressure. 100 mL of DDW was added to dissolve the residue and pH value was adjusted to 2 with addition of 2.0 M HCl solution. The reactant was extracted with 30 mL of chloroform three times. The organic phases were combined and washed several times with 100 mL DDW until the water layer is neutral. The organic layer was dried against anhydrous sodium sulfate. After filtration, the organic phase was concentrated to 10 ml. The residue was precipitated upon addition of 50 mL absolute ethyl ether. The white solid was obtained after filtration, washing with ethyl ether and drying under vacuum. Yield: 72.2%. Average molecular weight (Mw: 2475 Dalton. Mz/Mw=1.037).

2.4. Interaction between BSA and mPEG-OA. The stock solutions of 20 μM BSA and 1.2 mM mPEG-OA were prepared in water. The working solution for CD measurement was prepared with phosphate buffer solution (0.05 M, pH 7.40), the other working solutions were prepared with Tris-HCl buffer solution (0.01M Tris, 0.15 M NaCl, pH 7.40). Ketoprofen and ibuprofen stock solutions were prepared by dissolving them in a small amount of methanol and diluting with DDW to obtain 2.0 mM.

For the fluorescence measurement, 3.0 mL of 4.0 μM BSA solution was added to a 1.0 cm quartz cell. And then, 10 μL of mPEG-OA stock solution was successively added to the above BSA solution to make the solution concentrations of mPEG-OA in the range of 0.0 to 48 μM. The mixture solution was incubated for 10 min at designated temperature prior to scanning. Fluorescence quenching spectra of BSA were recorded from 300 to 500 nm using the excitation wavelength of 280 nm at three different temperatures (293, 303, and 313K), respectively. The corresponding synchronous fluorescence spectra were also scanned from 220 to 340 nm ($\Delta\lambda$ = 60 nm) and from 250 to 325 nm ($\Delta\lambda$= 15 nm), respectively.

FTIR measurements were carried out via the attenuated total reflection (ATR) method with a resolution of 4 cm-1 and accumulation of 120 scans at room temperature. The FTIR spectra of BSA, mPEG-OA, and mPEG-OA plus BSA solutions were recorded from 1800 to 1400 cm^{-1}, respectively. Then the FTIR spectrum of Tris-HCl buffer solution was also scanned, which was subtracted to obtain the corresponding FTIR spectra of above three sample solutions.

The CD spectra of BSA solution in the absence and presence of mPEG-OA were recorded at 0.1 nm intervals and averaged with three scans in the range of 202–250 nm at room temperature under constant nitrogen flush. The molar ratios of mPEG-OA to BSA were 0:1 and 20:1. The absorption spectra of BSA solution in the absence and presence of mPEG-OA were obtained in the range of 300–500 nm with the slit width of 1 cm.

The displacement experiments were conducted using the site probes, phenylbutazone and ibuprofen at the constant concentration of BSA and mPEG-OA. The mole ratio of mPEG-OA to BSA was set at 5:1 to eliminate the non-specific binding of probe. The fluorescence spectra of the above mixed solution titrated with ibuprofen and phenylbutazone were recorded upon excitation at 280 nm, respectively.

3. RESULTS SECTION

3.1. Synthesis and characterization of mPEG-OA. mPEG-OA was prepared through an esterification reaction between OA and mPEG as illustrated in Figure 1. Theoretically, the hydroxyl group of mPEG can directly esterify with carboxyl group of OA to prepare mPEG-OA, due to the presence of both hydroxyl group and carboxyl group in OA. However, according to the result of pre-experiments, direct esterification between OA and mPEG is more difficult with low yield and low conversion rate. This is probably caused by the great steric hindrance of the carboxyl group of OA. Thus, succinic anhydride was used as a linker. MPEG-SA was firstly prepared and further converted to MPEG-SC in order to increase the reaction activity according to the reported as illustrated in Figure 1[21]. Thus, mPEG-OA was successfully prepared.

The molecular weight and molecular weight distribution of mPEG-OA were measured by GPC method at 25°C using tetrahydrofuran (THF) as eluent at a flow rate of 1.0 mL·min^{-1}. The GPC chromatogram of mPEG-OA was recorded (Figure 2A). The weight-average molecular weight (Mw) is 2475 with a narrow distribution (Mz/Mw=1.037). Thus, the GPC spectrum confirmed that mPEG was successfully chemically grafted to OA molecules rather than encapsulation of OA.

Both OA and mPEG-OA were found to have an obvious absorption at 207 nm (Figure 2B). This result also confirmed that OA was chemically linked with mPEG.

From the FTIR spectra of OA, mPEG, mPEG-BSA and mPEG-OA (Figure 2C), the characteristic absorption of ethoxy unit in mPEG were observed at 2888 cm^{-1} (C-H stretching vibration), 1467 cm^{-1} (C-H bending vibration) and 1113 cm^{-1} (C-O ether stretching vibration) [22]. In the FTIR spectrum of OA, 1697 cm^{-1} can be assigned to stretching vibrations of carboxyl group of OA. At the same time, the typical carbonyl group absorption peaks were observed at 1736 cm^{-1} and 1726 cm^{-1} in mPEG-SA and mPEG-OA, respectively, which can be ascribed to stretching vibrations of carboxyl group and carbonyl group in ester group. The ^{1}H NMR spectrum was also used to confirm the formation of PEG-OA. The characteristic peaks at 5.29~5.23 ppm relates to the protons in the carbon-carbon double bond in OA molecule. The chemical shift of 3.80~3.33 ppm is caused by -CH_2- protons in the structure of mPEG. The chemical shift at 2.98~2.65 ppm belongs to -CH_2- attached to carboxyl group. The chemical shift at 1.64~1.14 ppm and 0.99~0.77 ppm can be attributed to protons in methyl group and methylene groups in OA molecule, respectively.

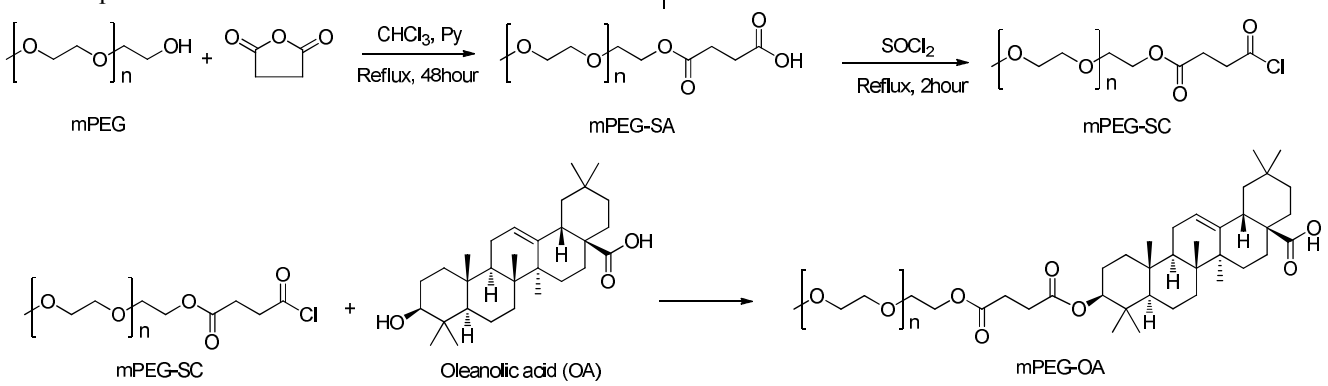

Figure 1. Synthesis diagram of mPEG-OA (n ≈ 44).

3.2. Fluorescence quenching of BSA by mPEG-OA. Although the intrinsic fluorescence of BSA can be caused by three fluorophores, tryptophan, tyrosine, and phenylalanine residues, Trp residues are more dominant as well as more sensitive to alteration in local environment [23]. So, the intrinsic fluorescence of Trp residues is often used for the analysis of drugs-BSA binding [20]. Fluorescence quenching refers to a process which decreases the fluorescence intensity of a fluorophore. A variety process during interactions can result in fluorescence quenching, including excited-state reactions, molecular rearrangements, energy transfer, ground-state complex formation and collisional quenching [17]. In this study, the fluorescence spectra of BSA can be quenched out by addition of mPEG-OA. The fluorescence spectra of BSA with different concentrations of mPEG-OA were recorded upon the excitation wavelength of 280 nm. As seen in Figure 3A, the fluorescence of BSA gradually decreased with the addition of PEG-OA, demonstrating that mPEG-OA could effectively quench the intrinsic fluorescence of BSA, however no significant shift of the emission maximum wavelength was observed. The process of fluorescence quenching can be classified into two types of static and dynamic. Dynamic quenching refers to a process that the fluorophore and the quencher come into contact during the lifetime of the excited state, whereas static quenching is fluorophore quencher complex formation. One way to discriminate static quenching from dynamic quenching is to examine their different dependence on temperature [24]. The dynamic quenching constant increases with increasing temperatures, because dynamic quenching is a diffusion process and higher temperatures will result in obvious increase of the diffusion coefficients. On the contrary, increased temperature likely decreases the stability of complexes and lower the static quenching constants [24].

In order to determine the fluorescence quenching type of the mPEG-OA□BSA system, the BSA fluorescence intensity data was analyzed by the Stern-Volmer equation as following [25].

$$\frac{F_0}{F} = 1 + K_{SV}[Q] \quad (1)$$

where F_0 and F are the fluorescence intensities of BSA solution at 346 nm in the absence and presence of mPEG-OA, respectively.

[Q] is the concentration of mPEG-OA and K_{sv} is the Stern-Volmer quenching constant. As depicted in Figure 3B, the plots of F_0/F against [mPEG-OA] at 293, 303 and 313K were fitted, respectively.

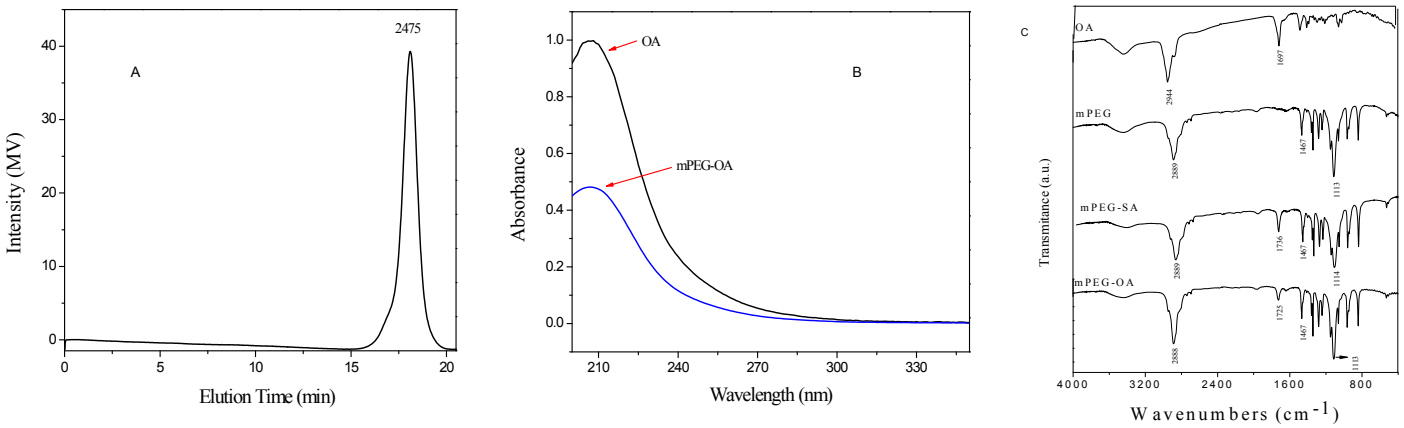

Figure 2. A. GPC chromatogram of the as-prepared mPEG-OA. B. UV absorption spectra of OA and mPEG-OA solutions. C. FTIR spectra of OA, mPEG, mPEG-A, and mPEG-OA samples.

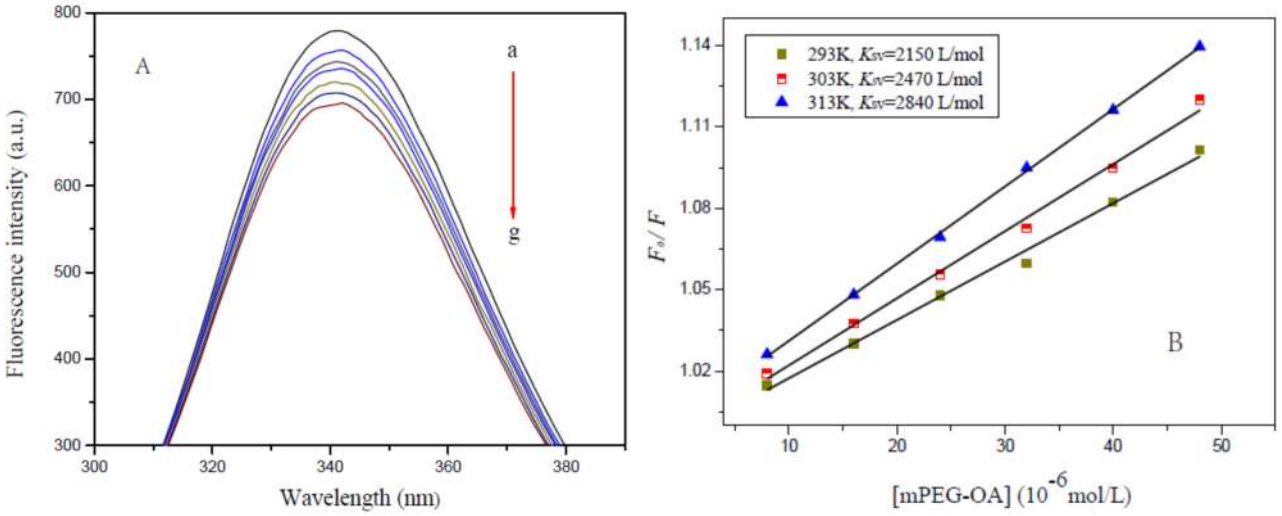

Figure 3. A. Fluorescence quenching spectra of BSA with an increase in mPEG-OA concentration. [BSA] = 4.0 μM; [mPEG-OA] (a→g) = 0, 8.0, 16.0, 24.0, 32.0, 40.0, and 48.0 μM; T=293K, pH=7.4. B. Stern–Volmer plots for the fluorescence quenching of BSA by mPEG-OA at three different temperatures. [BSA] = 4.0 μM; λem=346 nm.

As seen in Figure 3B, each plot exhibits a good linear relationship and the slopes of the Stern–Volmer plots increase with the temperature rising, implying that the fluorescence quenching of BSA by mPEG-OA should belong to a dynamic quenching process. It has been reported that quenching mechanism of BSA fluorescence by OA was a static quenching process through the formation of a ground-state complex [20]. In comparison with the interactions of OA and mPEG-OA with BSA, it can be inferred that mPEG unit plays a key role on the fluorescence quenching behavior of BSA caused by mPEG-OA.

To further confirm the quenching mechanism, the UV absorption spectra of BSA, mPEG-OA and BSA plus mPEG-OA solutions were recorded and the corresponding absorption spectra were obtained (Figure 4A). Obviously, the absorption spectra of BSA could be almost overlapped after adding different amounts of mPEG-OA. This result also supports the conclusion that the dynamic quenching during fluorescence quenching process of BSA caused by mPEG-OA.

3.3. Apparent association constant and number of binding sites. When small molecules bind independently to an equivalent site on a macromolecule (such as proteins), the equilibrium between free and complex molecules is achieved and can be described by the following equation:

$$\lg\frac{F_0 - F}{F} = \lg K_a + n\lg[Q] \qquad (2)$$

where K_a is apparent association constant, F_0 and F are the fluorescence intensities of BSA before and after addition of mPEG-OA, respectively, [Q] is the concentration of mPEG-OA, and *n* is number of binding site. According to Eq. (2), the values of K_a and *n* at 293, 303, and 313K were calculated from the intercept and slope values of each plot of $\lg(F_0 - F)/F$ versus lg[mPEG-OA] (Figure 4B) and summarized in Table 1. As seen from Table1，the values of all correlation coefficients are larger than 0.99, indicating that the interaction between mPEG-OA and BSA fits very well with the site-binding model underlined in Eq. (2). At the same time, the value of *n* approximately equal to 1 indicates that there is only one binding site on BSA involving in the binding process. In addition, the K_a values decrease with increasing temperature, implying that the ability of protein to store and transport drug will be impaired at high temperatures. Furthermore, the values of K_a do not reach the range of 10^4-10^6 L/mol, demonstrating that the interaction between mPEG-OA and BSA is not strong [26]. However, it was reported that the binding constant of OA with BSA was in the order of 10^4 L/mol [20]. This study indicated that mPEG modification weakens the binding affinity between OA and BSA. The reason is as follows. As seen from Figure 1, the structure of mPEG-OA containing both mPEG (hydrophilic part)

and OA group (hydrophobic part) simultaneously, shows the amphiphilic property, which allow mPEG-OA molecules to self-assemble micelles or vesicles in water solution. Thus, self-aggregation of mPEG-OA molecules prevents the approach to the surface of BSA molecules. As a result, the binding affinity between mPEG-OA and BSA is weakened comparing to that of OA [27].

3.4. The nature of the binding forces. The interaction forces between quencher and BSA comprises hydrophobic force, electrostatic interactions, van der Waals interactions and hydrogen bonds and so on [28]. In order to further clarify the interaction of mPEG-OA with BSA, the thermodynamic parameters were calculated. If the enthalpy change (ΔH) does not change significantly over the temperature range investigated, the values of enthalpy (ΔH) and entropy (ΔS) can be estimated from the van't Hoff equation [29]:

$$\ln K_a = -\frac{\Delta H}{RT} + \frac{\Delta S}{R} \qquad (3)$$

where ΔS is the entropy change; K_a is apparent association constant at corresponding temperatures and R is gas constant. The value of ΔH and ΔS can be obtained from the slope and intercept of the plot of ln K_a against 1/T, respectively (Figure 5A). Then the free energy change (ΔG) was estimated from the following equation:

$$\Delta G = \Delta H - T\Delta S \qquad (4)$$

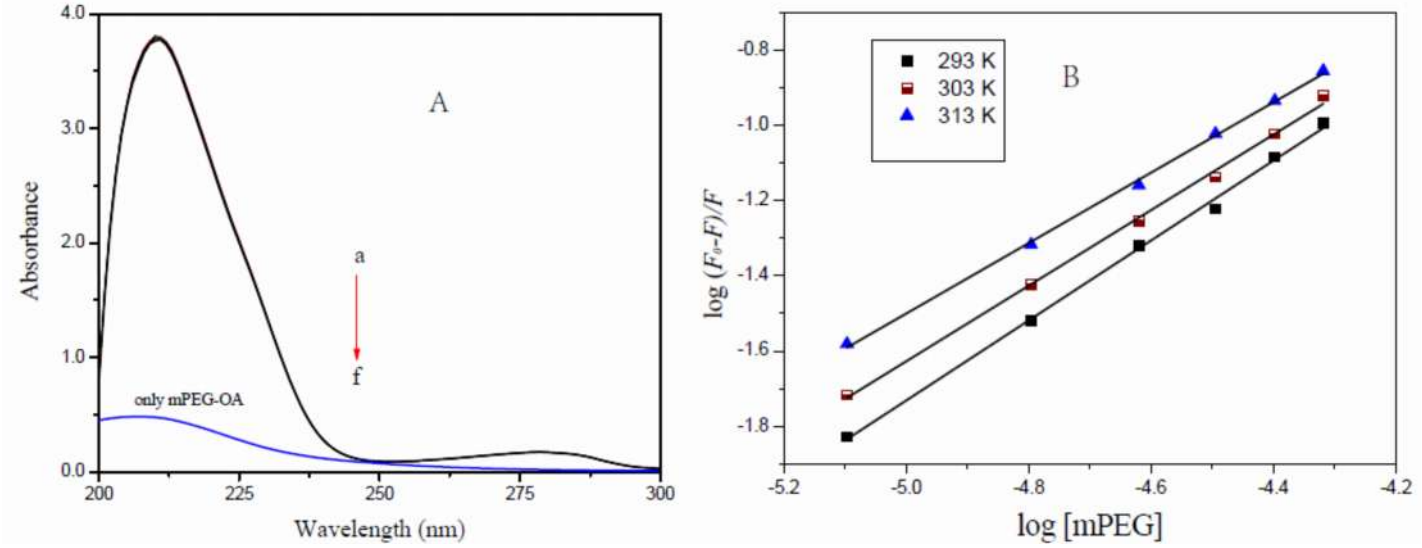

Figure 4. A. UV difference absorption spectra between BSA plus mPEG-OA and mPEG-OA solutions. [BSA] = 4.0 μM; [mPEG-OA] (a→f) = 0, 4.0, 8.0, 12.0, 20.0, and 32.0 μM. B. Plots of log (F_0-F)/F versus log [mPEG-OA] at different temperatures.

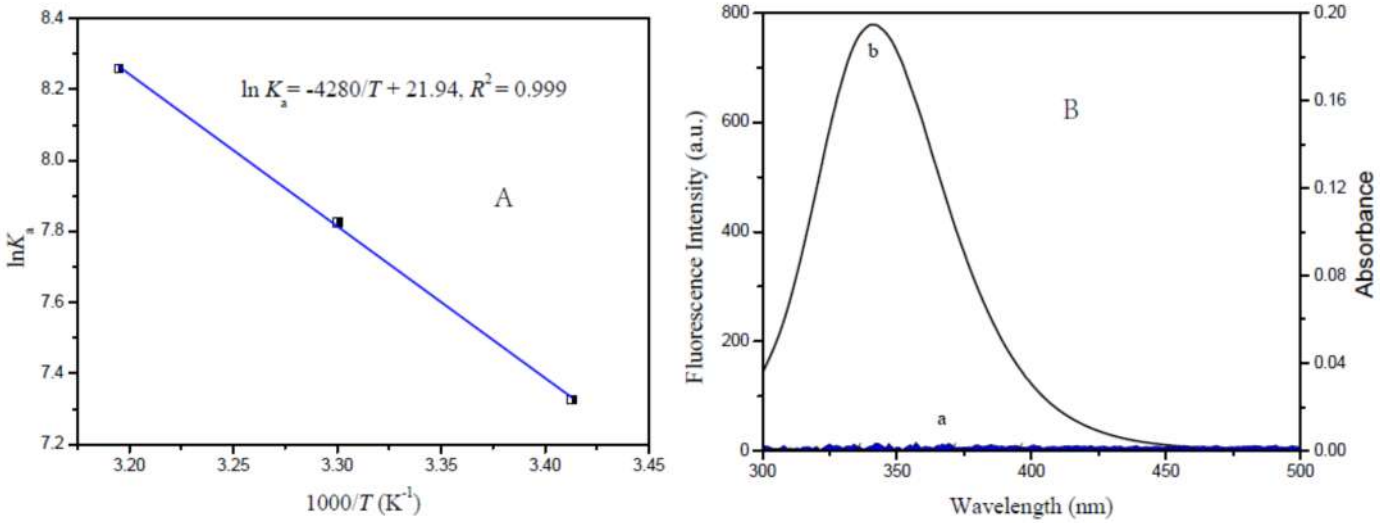

Figure 5. A. van't Hoff plot for the interaction between BSA and mPEG-OA. B. The spectral overlap of mPEG-OA absorption spectrum (a) with BSA fluorescence emission spectrum (b). [mPEG-OA] = [BSA]= 4.0 μM.

Table 1. The apparent association constants K_a, binding *number (n)* and the thermodynamic parameters for the mPEG-OA□BSA system at three different temperatures.

T (K)	*n*	K_a (L/mol)	R^{2a}	Δ*H* (kJ·mol^{-1})	Δ*S* (L·mol^{-1})	Δ*G* (kJ·mol^{-1})
293	1.06	3863	0.997			–17.86
303	1.00	2505	0.998	35.58	182.4	–19.69
313	0.94	1520	0.997			–21.51

[a] R^2 is the correlation coefficient.

The values of ΔH, ΔS and ΔG are summarized in Table 1. The negative value for free energy (ΔG) revealed that mPEG-OA binding to BSA is a spontaneous process. According to the rules for drug-protein interaction proposed by Ross and Subramanyam [28], the positive values of ΔH and ΔS for the mPEG-OA□BSA system reflect that the binding process is mainly entropy-driven and the enthalpy is unfavorable, and the hydrophobic forces plays an important role in the binding reaction of mPEG-OA with BSA [30].

3.5. Energy transfer from BSA to mPEG-OA. Fluorescence resonance energy transfer (FRET) as a powerful tool can be used for measuring the distance between donor and acceptor fluorophore in vitro and in vivo [31]. FRET is an electro-dynamic interaction between the electronic excited states of donor and acceptor molecules in which excitation is transferred from a donor molecule to an acceptor molecule. The FRET efficiency is dependent on following parameters: (i) the distance between donor and acceptor must be in the range of 2–8 nm; (ii) significant overlap between donor fluorescence and acceptor absorption bands; (iii) there must be a proper orientation of the transition dipole of the donor and acceptor. The distance between the ligand and the tryptophan residues in the protein are frequently evaluated according to the theory of Forster non-radiative energy transfer [31]. The efficiency of energy transfer (E) between the donor and acceptor could be calculated by the following equation.

$$E = 1 - \frac{F}{F_0} = \frac{R_0^6}{(R_0^6 + R^6)} \qquad (5)$$

where E is the efficiency of energy transfer, and R_0 is the critical distance as the efficiency of energy transfer is 50 %. The value of R_0^6 can be estimated according to the following equation.

$$R_0^6 = 8.8 \times 10^{-25}(Jk^2\varphi\eta^{-4}) \qquad (6)$$

where k^2 is the spatial orientation factor and value is 2/3; η is the averaged refracted index of the medium; φ is the fluorescence quantum yield of the donor; and J is degree of spectral overlap between the donor emission and the acceptor absorption. The value of J can be calculated using the following equation:

$$J = \frac{\int_0^\infty F(\lambda)\varepsilon(\lambda)\lambda^4 d\lambda}{\int_0^\infty F(\lambda)d\lambda} \qquad (7)$$

where F(λ) is the fluorescence intensity of the fluorescent donor at wavelength λ and ε(λ) is the molar absorption coefficient of the acceptor at wavelength of λ. Spectral overlap between the fluorescence emission spectrum of BSA and the UV–vis absorption spectrum of mPEG-OA is depicted in Figure 5B. In the present case, the values of *n* and φ are 1.36 and 0.15, respectively [32]. J=7.1401 × 10^{-16} $cm^3 \cdot L \cdot mol^{-1}$, *E* = 1.0%, R_0= 1.6 nm, and r = 3.5 nm were successively calculated using Eq. (5) to (7). Therefore, it was predicted that the energy transfers from BSA to mPEG-OA with high probability, since the values of r was less than 8 nm. This indicated that there was FRET occurring during the dynamic quenching [33].

3.6. The displacement experiments of site probes. BSA has a limited number of binding sites for endogenous and exogenous ligands, which are typically bound reversibly. When two ligands (denoted with L_1 and L_2) simultaneously bind to BSA, there are mainly two types of binding process as follows:

(1) competitive binding

$$L_1 \xrightarrow{+BSA} L_1 - BSA \xrightarrow{+L_2} L_2 - BSA + L_1$$

(2) non-competitive binding

$$L_1 \xrightarrow{+BSA} L_1 - BSA \xrightarrow{+L_2} L_2 - BSA - L_1$$

In order to identify the binding site of mPEG-OA on BSA, the competition displacement experiments were performed with two different site probes, phenylbutazone for site I and ibuprofen for site II, respectively. The percentage of fluorescence probe displaced by mPEG-OA was determined by measuring the changes in fluorescence intensity according to the method proposed by Sudlow and his co-workers [34].

$$Displacement(\%) = F_2 / F_1 \times 100\% \qquad (8)$$

where F_1 and F_2 denote the fluorescence intensity of BSA plus mPEG-OA mixture solution with and without the probe, respectively.

Based on the spectral data, the plots of F_2/F_1 against site probe concentration were fitted. As seen in Figure 6A, the fluorescence intensity was remarkably affected by addition of phenylbutazone. On the contrary, the addition of ibuprofen to the same solution had less effect on the fluorescence intensity of BSA. These results show that both mPEG-OA and phenylbutazone competitively bind to the same site in BSA. Hence, it can be concluded that sub-domain II A (site I) of BSA is the primary binding site for mPEG-OA on BSA, namely, nearby Trp-212 residue [35].

3.7. FTIR spectra of BSA. FTIR spectroscopy is often used to probe the secondary structural changes of proteins after its binding with ligands. In the FTIR spectra of proteins, amide I band (the C=O stretching of the polypeptide backbone) and amide II band have been widely acknowledged as the typical absorption peaks, and they mainly appear in the region of 1600–1700 cm^{-1} and 1500–1600 cm^{-1}, respectively. Both amide I band and amide II band have relationship with the secondary structure of the protein. However, amide I band is more sensitive to changes in the protein secondary structure compared to amide II [36].

In the present study, FTIR spectra of BSA solution and BSA plus mPEG-OA at different concentration were recorded (Figure 6B). No obvious shift in the peak positions for both amides I and II bands was observed upon adding mPEG-OA, proving that the protein secondary structure did not change in the presence of mPEG-OA.

3.8. CD spectra of BSA. To further investigate whether any conformational changes of BSA molecules occur in the binding process, the CD spectra of BSA solution with and without mPEG-OA were recorded (Figure 7A). The CD spectra of serum albumin exhibit two negative bands in the far-UV region at 208 and 222 nm, which are corresponding to characteristic of an α-helical

structure of protein [37]. The intensities of two bands reflect the amount of α-helicity of BSA. The CD results were expressed in terms of mean residue ellipticity (MRE) in deg·cm^2·dmol^{-1} according to the following equation [39].

$$\mathrm{MRE} = \frac{\text{Observed CD (mdeg)}}{C_P n l \times 10} \quad (9)$$

where C_p is the molar concentration of the BSA, n is the number of amino acid residues and l is the path length. The α-helix contents of BSA were calculated from MRE values at 208 nm using the following equation [38]:

$$\alpha\text{-Helix}\,(\%) = \frac{-\mathrm{MRE}_{208} - 4000}{33{,}000 - 4000} \times 100 \quad (10)$$

where MRE_{208} is the observed MRE value at 208 nm, 4000 is the MRE value of the β-form and random coil conformation cross at 208 nm and 33,000 is the MRE value of a pure α-helix at 208 nm. According to Eq. (9) and (10), the α-helicity content in the secondary structure of BSA in free BSA solution and mPEG-OA+BSA mixture solution was calculated to be 52.4% and 49.6%, respectively.

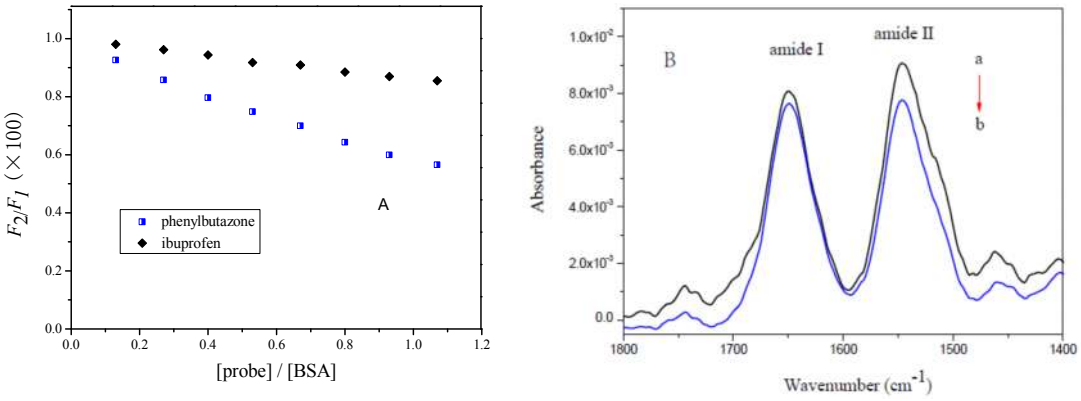

Figure 6. A. Effects of site maker probes on the fluorescence of the mPEG-OA–BSA system. [BSA] = 4.0 μM, [mPEG-OA] = 40 μM. B. FTIR spectrum of free BSA with different concentration of BSA at room temperature. [BSA] = 4.0 μM; [mPEG-OA](a→b) = 0 and 12.0 μM.

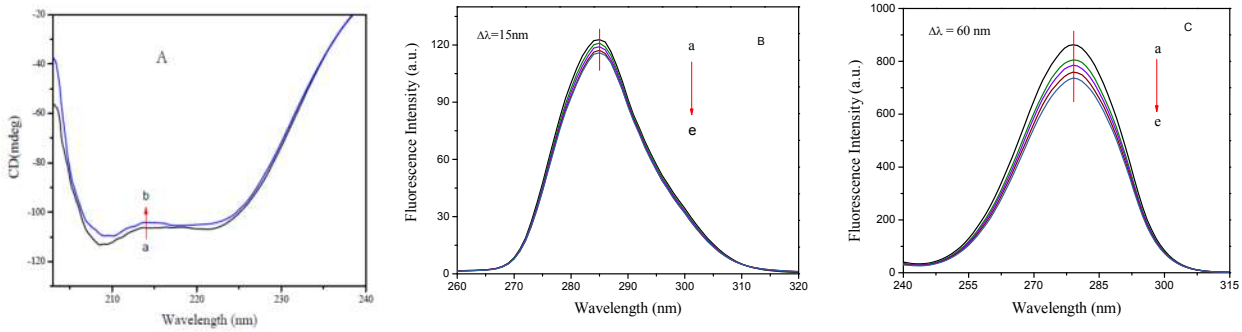

Figure 7. A. The CD spectra of BSA in the absence and presence of mPEG-OA. [BSA] = 1.0 μM; [mPEG-OA] (a→b) = 0 and 20 μM. B and C. The synchronous fluorescence spectra of BSA with different concentrations of mPEG-OA at 293 K. [BSA]=4.0 μM; [mPEG-OA] (a→e) = 0, 32.0, 48.0, 64.0, and 80.0 μM.

Therefore, the CD spectra of BSA indicate that the structure of BSA is predominantly α-helical before and after adding mPEG-OA. A decrease of 2.8% around in the α-helicity content at such high molar ratio of mPEG-OA to BSA implies that mPEG-OA bound to BSA did not cause a significant perturbation on the protein secondary structure at the concentration of mPEG-OA ranged from 0 to 48 □M. This result is consistent with the results of FTIR spectra analysis.

3.9. Synchronous fluorescence spectra of BSA. The synchronous fluorescence spectroscopy is often used to probe the conformational changes of proteins [39]. The micro-environmental changes of Trp and Tyr residues in BSA can be assessed by measuring their synchronous fluorescence spectra. The shift of maximum emission wavelength is closely related to change of polarity of chromophore [41]. When Δλ between excitation wavelength and emission wavelength was fixed at 15 or 60 nm, the synchronous fluorescence will provide the characteristic information of Tyr or Trp residues in BSA, respectivly [40].

Figure 7B shows the synchronous fluorescence spectra of BSA with mPEG-OA at different concentrations. It can be observed that fluorescence intensities of Trp and Tyr residues decreased with increasing mPEG-OA concentration, but the fluorescence emission peak position of Trp or Tyr residues did not show any significant shift, demonstrating that the polarity of the region around Trp or Tyr residues remained unchangeable after adding different amounts of mPEG-OA.

4. CONCLUSIONS

In this paper, water soluble mPEG–OA was successfully synthesized, and then its interaction with BSA was investigated via multiple spectroscopic techniques. The results show that mPEG-OA quenched the fluorescence of BSA via dynamic quenching mechanism and there was a low binding affinity between the drug and protein. The values of thermodynamic

parameters suggest that hydrophobic forces played a major role in the binding process. The value of binding distance r discloses that the energy transfers from BSA to mPEG-OA took place. The displacement experiments demonstrate that mPEG-OA was mainly situated in site I of BSA. The analysis of fluorescence quenching, CD and FTIR spectra indicate that addition of mPEG-OA did not cause obvious conformational changes of protein. This study is expected to provide useful information in the screening and designing of OA derivatives.

5. REFERENCES

[1] Shanmugam MK, Dai X, Kumar AP, Tan BK, Sethi G, Bishayee A., Oleanolic acid and its synthetic derivatives for the prevention and therapy of cancer: preclinical and clinical evidence, *Cancer letters*, 346, 2, 206-16, **2014.**

[2] Huang D, Ding Y, Li Y, Zhang W, Fang W, Chen X., Anti-tumor activity of a 3-oxo derivative of oleanolic acid, *Cancer letters*, 233, 2, 289-96,**2006.**

[3] Pollier J, Goossens A., Oleanolic acid, *Phytochemistry*, 77:10-5, **2012.**

[4] Tong HH, Wu HB, Zheng Y, Xi J, Chow AH, Chan CK., Physical characterization of oleanolic acid nonsolvate and solvates prepared by solvent recrystallization, *International journal of pharmaceutics*, 355, 1-2, 195-202, **2008.**

[5] Jeong DW, Kim YH, Kim HH, Ji HY, Yoo SD, Choi WR, et al. Dose-linear pharmacokinetics of oleanolic acid after intravenous and oral administration in rats, *Biopharmaceutics & drug disposition*, 28, 2, 51-57, **2007.**

[6] Liu J. Oleanolic acid and ursolic acid: research perspectives, *Journal of ethnopharmacology*,100, 1-2, 92-94, **2005.**

[7] Bailon P, Won CY. PEG-modified biopharmaceuticals, *Expert opinion on drug delivery*, 6, 1, 1-16, **2009.**

[8] Zhang X, Wang H, Ma Z, Wu B. Effects of pharmaceutical PEGylation on drug metabolism and its clinical concerns. *Expert opinion on drug metabolism & toxicology*, 10, 12, 1691-1702, **2014.**

[9] Olson RE, Christ DD. Chapter 33. Plasma Protein Binding of Drugs. *Annual Reports in Medicinal Chemistry*, 31, 327-36, **1996.**

[10] Kandagal PB, Ashoka S, Seetharamappa J, Shaikh SM, Jadegoud Y, Ijare OB. Study of the interaction of an anticancer drug with human and bovine serum albumin: spectroscopic approach. *Journal of pharmaceutical and biomedical analysis*. 41, 2, 393-9, **2006.**

[11] Li X, Mu J, Liu F, Tan EW, Khezri B, Webster RD, et al. Human transport protein carrier for controlled photoactivation of antitumor prodrug and real-time intracellular tumor imaging. *Bioconjugate chemistry*, 26, 5, 955-61, **2015.**

[12] Timerbaev AR, Hartinger CG, Aleksenko SS, Keppler BK. Interactions of antitumor metallodrugs with serum proteins: advances in characterization using modern analytical methodology. *Chemical reviews*. 106, 6, 2224-2248, **2006.**

[13] Saeidifar M, Mansouri-Torshizi H. Investigation of the Interaction Between Human Serum Albumin and Antitumor Palladium(II) Complex Containing 1,10-Phenanthroline and Dithiocarbamate Ligands. *Nucleosides, Nucleotides and Nucleic Acids*, 34, 1, 16-32, **2015.**

[14] Shang S, Liu Q, Gao J, Zhu Y, Liu J, Wang K, et al. Insights into In Vitro Binding of Parecoxib to Human Serum Albumin by Spectroscopic Methods. *Journal of Biochemical and Molecular Toxicology*. 28, 10, 433-441, **2014.**

[15] Yamasaki K, Maruyama T, Kragh-Hansen U, Otagiri M. Characterization of site I on human serum albumin: concept about the structure of a drug binding site. *Biochimica et Biophysica Acta (BBA) - Protein Structure and Molecular Enzymology*. 1295, 2, 147-57, **1996.**

[16] Manouchehri F, Izadmanesh Y, Ghasemi JB. Characterization of the interaction of glycyrrhizin and glycyrrhetinic acid with bovine serum albumin by spectrophotometric-gradient flow injection titration technique and molecular modeling simulations. *International Journal of Biological Macromolecules*. 102, 92-103, **2017.**

[17] Guo X, Hao A, Wu Q, Diao X, Liu W, Cong C, et al. Binding nature and conformational alternations of bovine serum albumin upon interaction with synthesized LaF3:Ce,Tb luminescent nanocrystals using multi-spectroscopic approach. *Journal of Luminescence*, 178, 210-218, **2016.**

[18] Naseri A, Hosseini S, Rasoulzadeh F, Rashidi M-R, Zakery M, Khayamian T. Interaction of norfloxacin with bovine serum albumin studied by different spectrometric methods; displacement studies, molecular modeling and chemometrics approaches. *Journal of Luminescence.* 157, 104-12, **2015.**

[19] Zacchigna M, Cateni F, Drioli S, Procida G, Altieri T. PEG–Ursolic Acid Conjugate: Synthesis and In Vitro Release Studies. *Scientia Pharmaceutica*. 82, 2, 411-21. **2014.**

[20] Cheng Z, Zhang Y. Fluorometric investigation on the interaction of oleanolic acid with bovine serum albumin. *Journal of Molecular Structure*, 879, 1–3, 81-87, **2008.**

[21] Porjazoska A, Yilmaz OK, Baysal K, Cvetkovska M, Sirvanci S, Ercan F, et al. Synthesis and characterization of poly(ethylene glycol)-poly(D,L-lactide-co-glycolide) poly(ethylene glycol) tri-block co-polymers modified with collagen: a model surface suitable for cell interaction. *Journal of biomaterials science Polymer edition*, 17, 3, 323-40, **2006.**

[22] Büyükyağcı A, Tuzcu G, Aras L. Synthesis of copolymers of methoxy polyethylene glycol acrylate and 2-acrylamido-2-methyl-1-propanesulfonic acid: Its characterization and application as superplasticizer in concrete. *Cement and Concrete Research*, 39, 7, 629-35, **2009.**

[23] Ghosh K, Rathi S, Arora D. Fluorescence spectral studies on interaction of fluorescent probes with Bovine Serum Albumin (BSA). *Journal of Luminescence,* 175, 135-40, **2016.**

[24] Bardajee GR, Hooshyar Z. Probing the interaction of a new synthesized CdTe quantum dots with human serum albumin and bovine serum albumin by spectroscopic methods. **Materials Science and Engineering: C**., 62, 806-815, **2016.**

[25] Lakowicz JR. Quenching of Fluorescence. In: Lakowicz JR, editor. *Principles of fluorescence spectroscopy*. second ed. New York: Plenum Press; p. 237-65, **1999.**

[26] Shiri F, Shahraki S, Shahriyar A, Majd MH. Exploring isoxsuprine hydrochloride binding with human serum albumin in the presence of folic acid and ascorbic acid using multispectroscopic and molecular modeling methods. *Journal of Photochemistry and Photobiology B: Biology.* 170, 152-163, **2017.**

[27] Yu M, Ding Z, Jiang F, Ding X, Sun J, Chen S, et al. Analysis of binding interaction between pegylated puerarin and bovine serum albumin by spectroscopic methods and dynamic light scattering. *Spectrochimica Acta Part A: Molecular and Biomolecular Spectroscopy*, 83, 1, 453-60, **2011.**

[28] Ross PD, Subramanian S. Thermodynamics of protein association reactions: forces contributing to stability. **Biochemistry**, 20, 11, 3096-3102, **1981.**

[29] Mathew M, Sreedhanya S, Manoj P, Aravindakumar CT, Aravind UK. Exploring the Interaction of Bisphenol-S with Serum Albumins: A Better or Worse Alternative for Bisphenol A? *The Journal of Physical Chemistry B,* 118, 14, 3832-43, **2014.**

[30] Ashoka S, Seetharamappa J, Kandagal PB, Shaikh SMT. Investigation of the interaction between trazodone hydrochloride and bovine serum albumin. *Journal of Luminescence*.;121, 1, 179-186, **2006.**

[31] Forster T. Part III: Action of light and Organic crsytals. In: Sinanoğlu O, editor. *Modern Quantum Chemistry: (Istanbul lectures).* New York: Academic press, pp. 93 – 137, **1966.**

[32] Cyril L, Earl JK, Sperry WM. *Biochemists' Handbook*. London: E. & F.N. Spon Ltd.; 84 p. **1961.**

[33] Hao C, Xu G, Feng Y, Lu L, Sun W, Sun R. Fluorescence quenching study on the interaction of ferroferric oxide nanoparticles with bovine serum albumin. *Spectrochimica Acta Part A: Molecular and Biomolecular Spectroscopy*. 184, 191-197, **2017.**

[34] Sudlow G, Birkett DJ, Wade DN. Further characterization of specific drug binding sites on human serum albumin. *Molecular pharmacology*, 12, 6, 1052-61, **1976.**

[35] Maciazek-Jurczyk M. Phenylbutazone and ketoprofen binding to serum albumin. Fluorescence study. *Pharmacological reports: PR.* 66, 5, 727-731, **2014.**

[36] Naik KM, Nandibewoor ST. Spectral characterization of the binding and conformational changes of bovine serum albumin upon interaction with an anti-fungal drug, methylparaben. *Spectrochimica Acta Part A: Molecular and Biomolecular Spectroscopy*, 105. 418-23, **2013.**
[37] Zhu L, Li G, Zheng F. Interaction of bovine serum albumi with two alkylimidazolium-based ionic liquids investigated by microcalorimetry and circular dichroism. *Journal of Biophysical Chemistry*, 2, 147-152, **2011.**
[38] Shi JH, Pan DQ, Jiang M, Liu TT, Wang Q. Binding interaction of ramipril with bovine serum albumin (BSA): Insights from multi-spectroscopy and molecular docking methods. *Journal of photochemistry and photobiology B, Biology*. 164, 103-11, **2016.**
[39] Bobone S, van de Weert M, Stella L. A reassessment of synchronous fluorescence in the separation of Trp and Tyr contributions in protein emission and in the determination of conformational changes. *Journal of Molecular Structure*, 1077, 68-76, **2014.**
[40] Selva Sharma A, Anandakumar S, Ilanchelian M. A combined spectroscopic and molecular docking study on site selective binding interaction of Toluidine blue O with Human and Bovine serum albumins. *Journal of Luminescence*, 151, 206-18, **2014.**

6. ACKNOWLEDGEMENTS

We acknowledge the financial support of Liaoning provincial department of education innovation team projects (Grant no. LT2012001), Shenyang science and technology plan project (Grant no. F13289100) and China Association for medical education (2016SKT-M019).